Development of tungsten fiber-reinforced tungsten with a porous matrix

Y Mao[1,5] ⓘ, J W Coenen[1] ⓘ, S Sistla[2], X Tan[3], J Riesch[4] ⓘ, L Raumann[1], D Schwalenberg[1], T Höschen[4], C Chen[3], Y Wu[3], C Broeckmann[2] and Ch Linsmeier[1] ⓘ

[1] Forschungszentrum Jülich GmbH, Institut für Energie-und Klimaforschung—Plasmaphysik, Partner in the Trilateral Euregio Cluster, 52425 Jülich, Germany
[2] Institut für Werkstoffanwendungen im Maschinenbau (IWM), RWTH Aachen University, 52062 Aachen, Germany
[3] School of Materials Science and Engineering, Hefei University of Technology, 230009 Hefei, People's Republic of China
[4] Max-Planck-Institut für Plasmaphysik, 85748 Garching b. München, Germany

E-mail: y.mao@fz-juelich.de

Abstract

Tungsten is the main candidate for the plasma-facing material in future fusion reactors. To overcome the brittleness of tungsten, tungsten fiber-reinforced tungsten (W_f/W) composites have been developed using a powder metallurgy process. In this study, a novel type of W_f/W with a porous matrix has been developed using field-assisted sintering technology. Compared with conventional W_f/W, the avoidance of a fiber–matrix interface simplified the production process. Initial mechanical testing showed that W_f/W with a porous matrix can establish a promising pseudo-ductile behavior with an increased fracture toughness compared with pure tungsten.

Keywords: tungsten, field-assisted sintering technology, porous matrix composites, fracture behavior

(Some figures may appear in colour only in the online journal)

1 Introduction

The extreme environment of the first wall of a fusion reactor puts unique challenges on materials and requires advanced mechanical and thermal properties. Tungsten is the main candidate for the plasma-facing material in fusion reactors [1, 2] as it is resilient against erosion, has the highest melting point of all metals and shows rather benign behavior under neutron irradiation [3]. However, the intrinsic brittleness of tungsten could cause some potential issues in the future fusion environment with high transient heat loads and neutron irradiation. To overcome this drawback, tungsten fiber-reinforced tungsten (W_f/W) composites have been developed, relying on an extrinsic toughening principle [4–8]. In recent studies, a process has been established to produce W_f/W using field-assisted sintering technology (FAST) [9–11]. FAST is a low-

voltage, pulsed direct current-activated, pressure-assisted sintering and synthesis technique. During this process, the fiber–powder mixture is consolidated to a bulk material by Joule heating under uniaxial pressure in a mold. With a weak oxide interface and high-strength tungsten fibers, a pseudo-ductile fracture behavior can be achieved, as demonstrated in previous studies [9, 12]. It has been reported that a relatively weak interface between the fiber and the matrix is beneficial for realizing pseudo-ductility of the composites [12–14]. The improved fracture resistance relies on the extra energy dissipation mechanisms such as interface debonding, crack bridging by the fibers and fiber pull-out.

However, some problems are potentially introduced by the inclusion of an oxide interface, for example interface delamination on the surface under exposure to a high heat flux [15]. What is more important, however, is that currently such interface production is very costly in terms of time and money due to the use of magnetron sputtering [12]. This is the
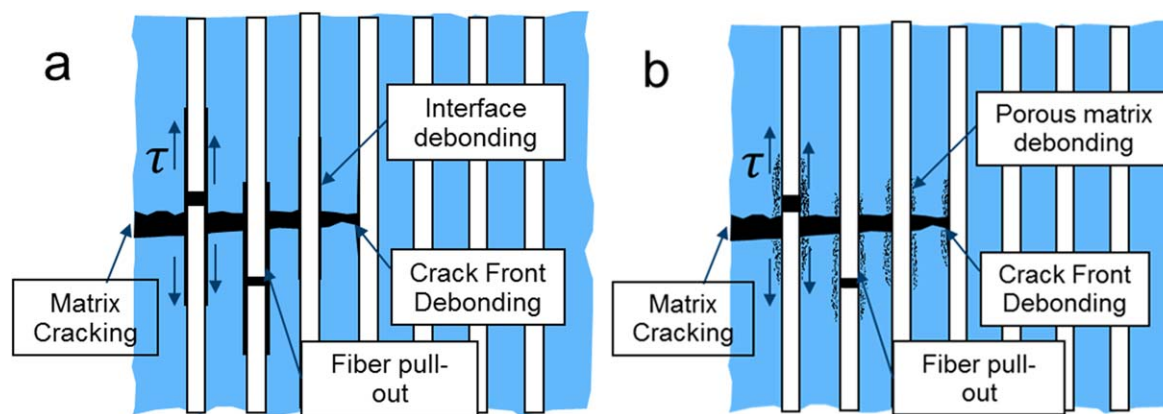
Figure 1. Schematics of the damage processes that enable damage tolerance in (a) conventional dense-matrix fiber-reinforced composites with a weak interface and (b) porous matrix fiber-reinforced composites without fiber coatings [17].

bottleneck in the production process of W_f/W. Other coating techniques are under investigation but are not yet feasible for short fibers. Therefore, it would be highly beneficial for large-scale production if the application of an interface can be avoided. Porous matrix composites offer a possible alternative to conventional weak interface composites.

2 Tungsten fiber-reinforced tungsten with a porous matrix

For fiber-reinforced composites with a brittle matrix, damage tolerance is obtained when the matrix acts as a mechanical 'buffer' between adjacent fibers so that the cracks from the matrix do not penetrate into the fibers. Fiber breakage should remain isolated with minimal stress concentration in neighboring fibers. It can be seen from previous studies of W_f/W [12] that if no interphase is applied between fiber and matrix the crack can easily penetrate through the fibers, and thus fracture resistance cannot be enhanced.

A buffer zone between fiber and matrix can be enabled in two ways. Conventionally, a fiber coating is used to promote crack deflection, fiber/matrix debonding and frictional sliding along the fiber–matrix interface (figure 1(a)). This principle was used in previous work on W_f/W [7, 12, 16]. Another approach involves the use of a controlled amount of fine-scale matrix porosity, obviating the need for fiber coating (figure 1(a)). This approach can be viewed as an extension of the weak coating concept. For this case, crack deflection occurs because of the low strength of the porous interphase and its poor cohesion with the fibers [17, 18]. This principle has also been widely used, for example in carbon fiber-reinforced carbon (CFC) or silicon carbide fiber-reinforced silicon carbide (SiC/SiC) [19].

In this study, the principle of a porous matrix composite is used in the design of W_f/W. A porous matrix is realized by reducing the sintering temperature during the FAST process. Another potential advantage of decreasing the process temperature is that fiber recrystallization and grain growth during sintering is mitigated. This is helpful for retaining good fiber mechanical properties [20, 21].

Table 1. FAST process parameters for conventional W_f/W and porous matrix W_f/W [12].

Sintering parameters	Conventional W_f/W	Porous matrix W_f/W
Temperature	1900 °C	1550 °C
Pressure	60 MPa	60 MPa
Time	4 min	4 min
Heating rate	100 °C min^{-1}	100 °C min^{-1}
Relative density	∼93%	∼88%
Fiber volume fraction	30%	40%
Fiber–matrix interlayer	With yttria interface	No yttria interface

3 Production process

Similar to conventional W_f/W production, the raw materials for fabrication of the porous matrix W_f/W are pure tungsten powders (provided by OSRAM GmbH) with an average particle size of 5 μm (Fischer subsieve size) and potassium-doped short tungsten fibers (provided by OSRAM GmbH) with length of 2.4 mm and diameter of 0.15 mm. The tungsten fibers were produced by a drawing process and then cut to the required length. Due to the drawn microstructure having elongated grains, the tungsten fibers have an extremely high tensile strength (∼3000 MPa) with ductile fracture behavior at room temperature [21, 22]. The aim of potassium doping is to endow the structure with advanced microstructural stability at high temperatures, since potassium (at about 75 ppm) is present in the form of nano-dispersed bubble rows along the elongated grains pinning the grain boundaries [21, 23].

During the production, the tungsten fibers were mixed with the tungsten powders by manual shaking in a vessel in order to obtain a random distribution of fibers. The fiber weight fraction in the mixture was 40%. For conventional W_f/W, yttrium oxide was used as the fiber–matrix interface. For the case of increasing fiber volume fraction, the weak yttrium oxide interface content will also be higher. If the weak layer content in the composites is too high, the strength of the material will decrease due to the early failure of the weak
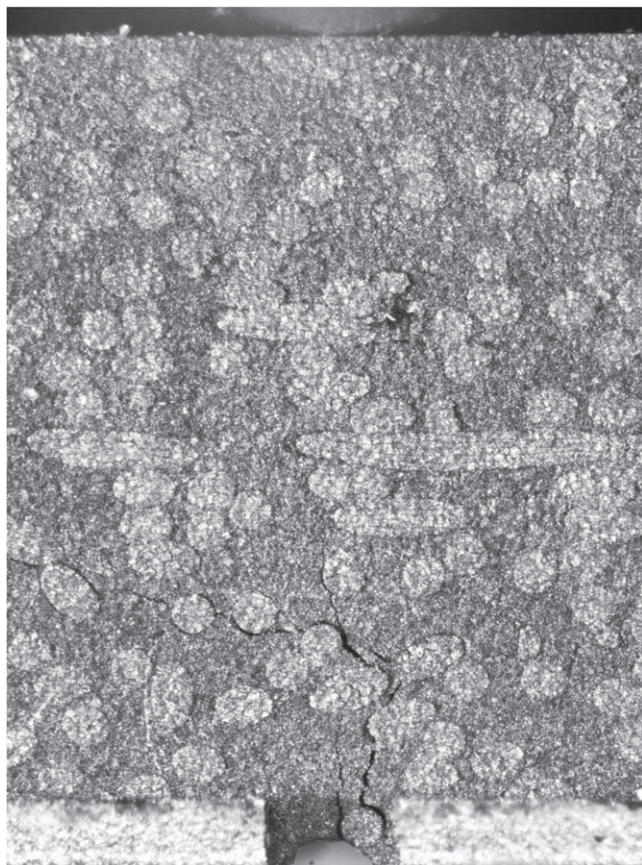
Figure 2. Image from the tracking camera during the bending test showing the crack length.

Figure 3. Force–displacement curves of porous matrix W_f/W compared with typical conventional W_f/W and pure tungsten.

Figure 4. Typical porous matrix W_f/W after the three-point bending test.

yttrium oxide [12]. Therefore, a fiber volume fraction of 30% is an optimized value balancing material strength and fracture behavior (this result will be publish in a later study). For porous matrix W_f/W, since no weak layer is involved, a higher fiber volume fraction can be applied. For other porous matrix composites, such as SiC/SiC or CFC, the fiber volume fraction is normally higher than 50% [17]. Therefore, for the first attempt a 40% fiber volume fraction was used for the porous matrix W_f/W.

The production parameters for the FAST process are shown in table 1, with the comparison with typical parameters used in the conventional W_f/W process [12]. During the FAST process, the powder–fiber mixture is consolidated in a graphite die with an inner diameter of 40 mm . Tungsten foil was used to separate the sample and the graphite mold in order to reduce carbon contamination [10, 24]. Based on the results in [24], if a tungsten foil is not added to separate the mold and the sample, carbon contamination will be detected in the tungsten fibers after the FAST process. Nanosized carbides in the grains and the carbide layer on the grain boundaries are formed during the production process. This carbon contamination will cause embrittlement of the tungsten fibers. Therefore, in recent research, tungsten foil protection was used in all W_f/W production by FAST. Sintering was performed under a va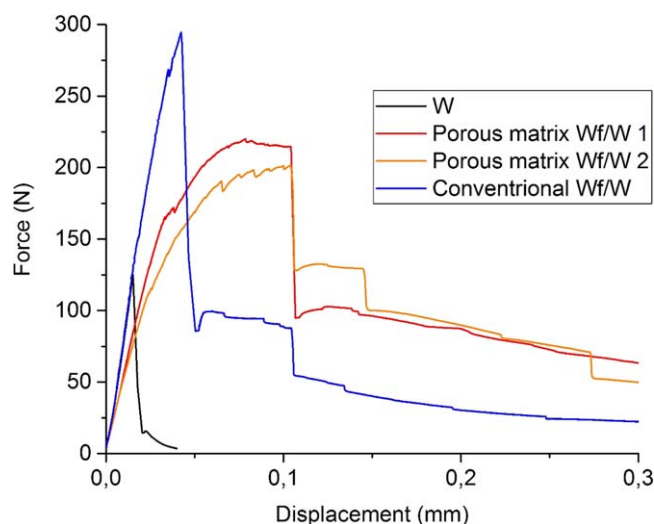cuum below 0.1 mbar. As result, a coin-shaped sample (40 mm diameter and $\sim$5 mm high) was produced. The relative density of the samples after sintering was around 88% according to the density measurement using Archimedes' principle.

4 Mechanical characterization and thermal diffusivity measurement

To study the fracture behavior of the porous matrix composites, an *in situ* three-point bending test was performed similar to the test in [25]. The samples were manufactured based on the EU standards DIN EN ISO 148-1 and 14556: 2006–10 [26]. The sample dimensions (KLST geometry) were as follows [27]: 3 mm × 4 mm × 27 mm, 22 mm span, 1 mm V-notch depth, 0.1 mm notch root radius, shaped by electrical discharge machining (EDM) without further surface or notch modification.

A universal testing device (TIRAtest 2820, no. R050/01, TIRA GmbH) with an optical camera system (DU657M, Toshiba) was used to perform the test. A displacement speed of $1 \mu m\,s^{-1}$ was used. The camera system tracked crack behavior and measured absolute sample movement. One typical tracking image taken during the experiment is shown in figure 2. From these data a force–displacement curve can be determined. The vertical movement of the sample relative to the reference stage is defined as the sample displacement.
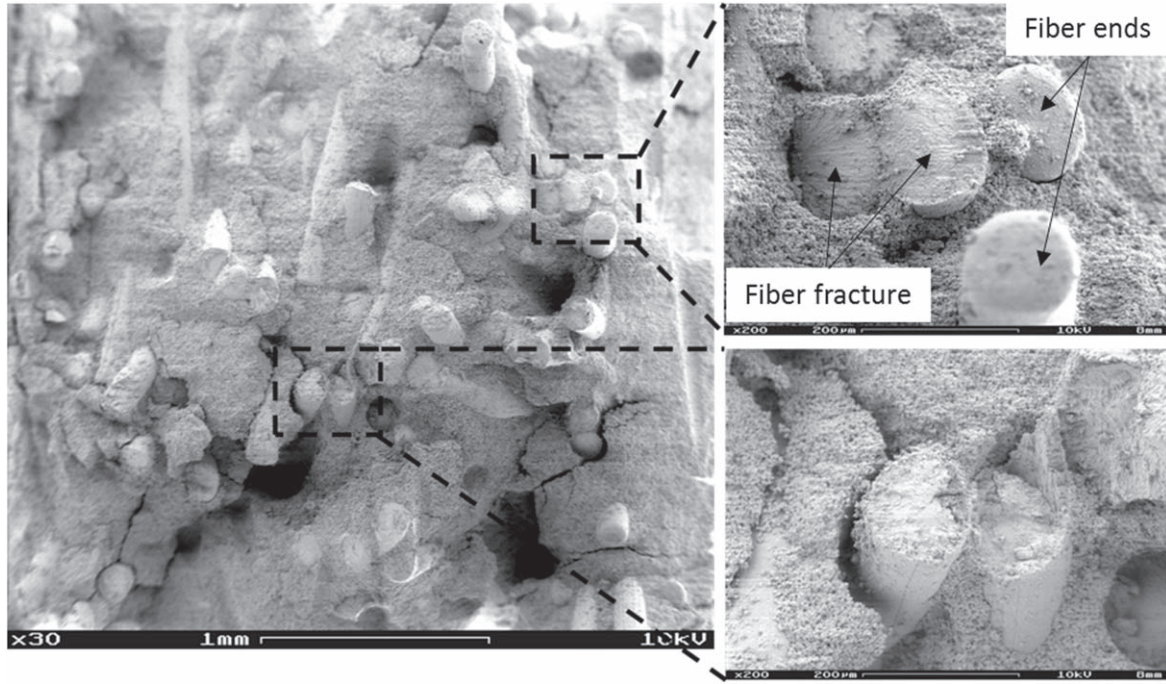
Figure 5. Fracture surface after three-point bending test.

Two samples were tested and compared with conventional W_f/W in a previous study [25].

Apart from a force–displacement curve, fracture toughness (K_q) can also be calculated based on the ASTM E399 standard:

$$K_q = \frac{PS}{BW^{3/2}} f(a_f/W) \qquad (1)$$

where P is the maximum load during stable crack growth, S is the distance between the support pins, B is the sample width, W is the sample thickness and a_f is the stable crack length, which is equal to the pre-notch length plus the crack extension length. The function $f(a_f/W)$ is described in ASTM E399 as:

$$f\left(\frac{a_f}{W}\right) =$$
$$\frac{3\left(\frac{a_f}{W}\right)^{\frac{1}{2}}\left\{1.99 - \left(\frac{a_f}{W}\right)\left(1 - \frac{a_f}{W}\right)\left(2.15 - \frac{3.93 a_f}{W} + \frac{2.7 a_f^2}{W^2}\right)\right\}}{2\left(1 + \frac{2a_f}{W}\right)\left(1 - \frac{a_f}{W}\right)^{\frac{3}{2}}}. \qquad (2)$$

In this study, the crack extension length (a_f) is measured from the *in situ* tracking image as the surface crack length. The corresponding force before the unstable load-drop is used as the maximum loading.

To investigate the influence of porosity on the thermal conductivity properties, thermal diffusivity measurement was performed from room temperature to 450 °C using a laser flash diffusivity system (LFA457, Germany). The specimen was a disc with a diameter of 6 mm and thickness of 2 mm. The testing atmosphere was Ar. For comparison, the thermal diffusivity of a conventional W_f/W sample [25] with ∼94% density, 30% fiber volume fraction and a 1.5 μm yttrium oxide fiber–matrix interface was also measured.

5 Results and discussions

The force–displacement curves of the porous matrix W_f/W during the three-point bending test are shown in figure 3. Typical force–displacement curves of conventional W_f/W and pure tungsten from a previous study are also included for comparison [25].

From figure 3 it can be seen that a pseudo-ductile behavior is established for both porous matrix W_f/W samples [12]: after linear-elastic deformation, the slope of the curve changes gradually to zero with several small load drops; then a massive load-drop occurs after the maximum force is reached; afterwards, the samples tend to have a stepwise or continuous load decrease. A typical sample overview after the three-point bending test is shown in figure 4. Even after large deformation (vertical bending displacement > 0.3 mm), the sample remains whole with a strength of over 50 N.

Compared with conventional W_f/W in figure 3 and typical samples in [25], the maximum loading is lower but the ability to deform before massive load-drop is greater. During the elastic deformation stage, the slope of the porous matrix W_f/W is lower than that of conventional W_f/W and pure tungsten. This effect can be attributed to its lower density.

Another noticeable point is that the strength–maximum loading of the porous matrix W_f/W is lower than that of conventional W_f/W due to the much weaker matrix. This is compromise that has to be made when using porous matrix composites: in the absence of fiber coatings, the matrix must be sufficiently weak to enable damage tolerance under fiber-dominated loadings. This weak matrix will reduce the strength properties of the material, but the decrease in strength could potentially be compensated by increasing the fiber volume fraction, which will be discussed in future work.

Table 2. Fracture toughness of porous matrix W_f/W compared with the results of a previous study on fracture toughness of W_f/W and polycrystalline tungsten [28].

Samples	Fracture toughness, K_q (MPa m$^{1/2}$)
Pure tungsten	5 ± 1
Conventional W_f/W	28 ± 9
Porous matrix W_f/W	30 ± 1
Polycrystalline tungsten (as sintered) [28]	5.1
Polycrystalline tungsten (rolled and drawn) [28]	35.1

To analyze the fracture surface, the sample in figure 4 was broken apart manually after the bending test. The scanning electron microscopy analysis of the fracture surface is shown in figure 5. The uneven topology of the surface is an indication of crack deflection. Additionally, debonding of the fiber–matrix interface is observed, and a notable fiber pull-out effect can also be seen. Some clear fiber end edges without fracture are also visible, indicating pull-out of the fiber-ends from the matrix.

Based on the quantitatively measured force–displacement curves and the tracking images during the test, fracture toughness (K_q) was calculated based on equation (1), similar to a previous study [25]. The results are shown in table 2, together with the fracture toughness of conventional W_f/W and pure tungsten produced by FAST from a previous study [25]. It is necessary to state that all the average fracture toughness' listed here are based on only a limited number of tests. Also, the sample is smaller than in the standard test. Therefore, large scattering of the results can be expected. However, from table 2 it is still safe to conclude that the fracture toughness of porous matrix W_f/W is much higher than that of pure tungsten and comparable to conventional W_f/W. Compared with the previous study on fracture toughness of polycrystalline tungsten [28], the porous matrix W_f/W has a comparable value to rolled and drawn tungsten.

Based on the results above, it can be concluded that porous matrix W_f/W shows a promising pseudo-ductile behavior with increased damage tolerance compared with pure tungsten. Similar to conventional W_f/W, fiber bridging, fiber pull-out, crack deflection and interface debonding are probably the energy dissipation mechanisms contributing to the elevated fracture resistance.

The thermal diffusivity of porous matrix W_f/W is shown in figure 6 in comparison with conventional W_f/W and reference pure tungsten [29]. It can be seen that both conventional W_f/W and porous matrix W_f/W show lower thermal diffusivity than reference tungsten, due to the higher porosity. The thermal diffusivity of porous matrix W_f/W is ~82% of the value for pure tungsten. This decrease of the thermal conductivity will indeed have some influence on the heat exhaust when W_f/W is used as a plasma-facing material. However, since the thermal conductivity of tungsten is already quite high, this decreased thermal conductivity is still acceptable when considering its improved mechanical
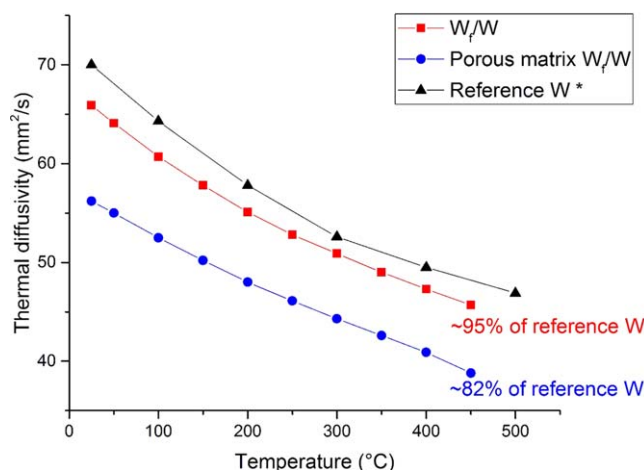
Figure 6. Thermal diffusivity of porous matrix W_f/W compared with conventional W_f/W and reference pure tungsten [29].

properties. Additionally, for the next step, the fiber volume fraction of porous matrix W_f/W will be optimized. When a higher fiber volume fraction is achieved, the density of porous matrix W_f/W will further be increased which will promote its thermal conductivity behavior.

6 Summary and outlook

In this work, porous matrix W_f/W was produced by FAST for the first time. Three-point bending tests were performed to understand the fracture behavior of the material. The results were compared with those for pure tungsten produced by FAST and conventional W_f/W. Based on the initial results, porous matrix W_f/W can achieve a promising defect tolerance. Compared with conventional W_f/W, the production process is much easier due to the omission of interface coating, which is a great benefit considering possible large-scale production in the near future.

For the next step, the porous matrix needs to be further optimized with the aim of achieving better material properties. The fiber volume fraction and sample density are the most critical points that need to be adjusted. Investigations are already being carried out in terms of these aspects and will be discussed in a future publication.

Apart from further optimization of the material properties, when porous matrix W_f/W is used as a plasma-facing component other properties need to be considered, such as hydrogen retention and oxidation behavior in case of an accidental air inrush. For hydrogen retention, based on the study in [6], the pores in W_f/W are mainly open pores. Therefore, a dramatic increase in hydrogen retention is not expected. The oxidation behavior of porous matrix W_f/W could be potentially improved by using the idea of a self-passivating tungsten alloy [30]. These points will be investigated in future studies.
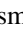
Acknowledgments

ORCID iDs

Y Mao ⬤ https://orcid.org/0000-0002-5518-2791
J W Coenen ⬤ https://orcid.org/0000-0002-8579-908X
J Riesch ⬤ https://orcid.org/0000-0001-6896-6352
Ch Linsmeier ⬤ https://orcid.org/0000-0003-0404-7191

References

[1] Philipps V 2011 Tungsten as material for plasma-facing components in fusion devices *J. Nucl. Mater.* **415** S2–9

[2] Coenen J W *et al* 2016 Materials for DEMO and reactor applications—boundary conditions and new concepts *Phys. Scr.* **T167** 014002

[3] Smid I, Akiba M, Vieider G and Plöchl L 1998 Development of tungsten armor and bonding to copper for plasma-interactive components *J. Nucl. Mater.* **258–63** 160–72

[4] Riesch J *et al* 2013 *In situ* synchrotron tomography estimation of toughening effect by semi-ductile fibre reinforcement in a tungsten-fibre-reinforced tungsten composite system *Acta Mater.* **61** 7060–7071.

[5] Gietl H 2018 Textile preforms for tungsten fibre-reinforced composites *J. Compos. Mater.* **52** 3875–84

[6] Mao Y *et al* 2019 Spark plasma sintering produced W-fiber-reinforced tungsten composites *Spark Plasma Sintering of Materials: Advances in Processing and Applications.* ed P Cavaliere (Berlin: Springer International Publishing) pp 239–61

[7] Gietl H, Riesch J, Coenen J W, Hoschen T, Linsmeier C and Neu R 2017 Tensile deformation behavior of tungsten fibre-reinforced tungsten composite specimens in as-fabricated state *Fusion Eng. Des.* **124** 396–400

[8] Du J, Höschen T, Rasinski M, Wurster S, Grosinger W and You J H 2010 Feasibility study of a tungsten wire-reinforced tungsten matrix composite with ZrO_x interfacial coatings *Compos. Sci. Technol.* **70** 1482–9

[9] Mao Y *et al* 2017 Development and characterization of powder metallurgically produced discontinuous tungsten fiber reinforced tungsten composites *Phys. Scr.* **T170** 014005

[10] Coenen J W *et al* 2018 Improved pseudo-ductile behavior of powder metallurgical tungsten short fiber-reinforced tungsten (Wf/W) *Nucl. Mater. Energy* **15** 214–9

[11] Coenen J W *et al* 2017 Advanced materials for a damage resilient divertor concept for DEMO: powder-metallurgical tungsten-fibre reinforced tungsten *Fusion Eng. Des.* **124** 964–8

[12] Mao Y *et al* 2018 Influence of the interface strength on the mechanical properties of discontinuous tungsten fiber-reinforced tungsten composites produced by field assisted sintering technology *Composites* A **107** 342–53

[13] Czél G and Wisnom M 2013 Demonstration of pseudo-ductility in high performance glass/epoxy composites by hybridisation with thin-ply carbon prepreg *Composites* A **52** 23–30

[14] Ming-Yuan H and Hutchinson J W 1989 Crack deflection at an interface between dissimilar elastic materials *Int. J. Solids Struct.* **25** 1053–67

[15] Coenen J W *et al* 2019 Materials development for new high heat-flux component mock-ups for DEMO *Fusion Eng. Des.* **146** 1431–6

[16] Du J, You J-H and Höschen T 2012 Thermal stability of the engineered interfaces in Wf/W composites *J. Mater. Sci.* **47** 4706–15

[17] Zok F W and Levi C G 2001 Mechanical properties of porous-matrix ceramic composites *Adv. Eng. Mater.* **3** 15–23

[18] Mackin T J, Yang J Y, Levi C G and Evans A G 1993 Environmentally compatible double coating concepts for sapphire fiber-reinforced γ-TiAl *Mater. Sci. Eng.* A **161** 285–93

[19] Brennan J J 2000 Interfacial characterization of a slurry-cast melt-infiltrated SiC/SiC ceramic-matrix composite *Acta Mater.* **48** 4619–28

[20] Riesch J *et al* 2016 Properties of drawn W wire used as high performance fibre in tungsten fibre-reinforced tungsten composite *IOP Conf. Ser.: Mater. Sci. Eng.* **139** 012043

[21] Riesch J *et al* 2016 Development of tungsten fibre-reinforced tungsten composites towards their use in DEMO-potassium doped tungsten wire *Phys. Scr.* **T167** 014006

[22] Zhao P *et al* 2017 Microstructure, mechanical behaviour and fracture of pure tungsten wire after different heat treatments *Int. J. Refract. Met. H* **68** 29–40

[23] Linsmeier C *et al* 2017 Development of advanced high heat flux and plasma-facing materials *Nucl. Fusion* **57** 092007

[24] Mao Y *et al* 2019 On the nature of carbon embrittlement of tungsten fibers during powder metallurgical processes *Fusion Eng. Des.* **145** 18–22

[25] Mao Y *et al* 2019 Fracture behavior of random distributed short tungsten fiber-reinforced tungsten composites *Nucl. Fusion* **59** 086034

[26] Rieth M and Hoffmann A 2010 Influence of microstructure and notch fabrication on impact bending properties of tungsten materials *Int. J. Refract. Met. Hard Mater* **28** 679–86.

[27] DIN 50115 1991 *Notched bar impact testing of metallic materials using test pieces other than ISO test pieces* (Berlin: Deutsches Institut fur Normung E V)

[28] Gludovatz B, Wurster S, Hoffmann A and Pippan R 2010 Fracture toughness of polycrystalline tungsten alloys *Int. J. Refract. Met. Hard Mater* **28** 674–8

[29] Habainy J, Dai Y, Lee Y and Iyengar S 2018 Thermal diffusivity of tungsten irradiated with protons up to 5.8 dpa *J. Nucl. Mater.* **509** 152–7

[30] Litnovsky A *et al* 2017 Smart alloys for a future fusion power plant: first studies under stationary plasma load and in accidental conditions *Nucl. Mater. Energy* **12** 1363–7